AGU ADVANCING EARTH AND SPACE SCIENCES

Geophysical Research Letters

RESEARCH LETTER
10.1029/2025GL118267

Modeling of Methyl Hydroperoxide Observations in Urban and Remote Air Over South Korea: Methylperoxy Radical Chemistry and Inference of Atmospheric Methanediol

L. H. Yang[1], D. J. Jacob[1,2], K. H. Bates[3], H. Lin[1], H. M. Allen[4], J.-F. Müller[5], S. S. Brown[6], R. Dang[1], N. K. Colombi[2], S. Zhai[7,8], R. M. Yantosca[1], J. F. Brewer[9], N. L. Ng[10,11,12], J. D. Crounse[13], P. O. Wennberg[13,14], K. Li[15], and H. Liao[15]

[1]School of Engineering and Applied Sciences, Harvard University, Cambridge, MA, USA, [2]Department of Earth and Planetary Sciences, Harvard University, Cambridge, MA, USA, [3]Department of Mechanical Engineering, University of Colorado Boulder, Boulder, CO, USA, [4]Laboratoire des Sciences du Climat et de l'Environnement, Université Paris-Saclay, Gif-sur-Yvette, France, [5]Department of Atmospheric Composition, Royal Belgian Institute for Space Aeronomy, Brussels, Belgium, [6]Chemical Sciences Division, Earth System Research Laboratory, National Oceanic and Atmospheric Administration, Boulder, CO, USA, [7]Department of Earth and Environmental Sciences, Faculty of Science, The Chinese University of Hong Kong, Hong Kong, China, [8]Institute of Environment, Energy and Sustainability, The Chinese University of Hong Kong, Hong Kong, China, [9]Department of Bioproducts and Biosystems Engineering, University of Minnesota, St. Paul, MN, USA, [10]School of Civil and Environmental Engineering, Georgia Institute of Technology, Atlanta, GA, USA, [11]School of Earth and Atmospheric Sciences, Georgia Institute of Technology, Atlanta, GA, USA, [12]School of Chemical and Biomolecular Engineering, Georgia Institute of Technology, Atlanta, GA, USA, [13]Division of Geological and Planetary Sciences, California Institute of Technology, Pasadena, CA, USA, [14]Division of Engineering and Applied Science, California Institute of Technology, Pasadena, CA, USA, [15]State Key Laboratory of Climate System Prediction and Risk Management/Collaborative Innovation Center of Atmospheric Environment and Equipment Technology, School of Environmental Science and Engineering, Nanjing University of Information Science and Technology, Nanjing, China

Abstract Methyl hydroperoxide (MHP) is produced by the $CH_3O_2 + HO_2$ reaction in the oxidation cascade of volatile organic compounds (VOCs). During KORUS-AQ (May–June 2016), aircraft observations over Seoul using chemical ionization mass spectrometry reported MHP concentrations exceeding 1 ppb in the planetary boundary layer, four times higher than simulated by the GEOS-Chem atmospheric chemistry model. We show that this discrepancy can be explained in part by the instrument's positive interference from methanediol (MD) under high-humidity conditions, where MD is produced in clouds by formaldehyde hydration. Including MD chemistry in GEOS-Chem increases the global formic acid source by 11% but has otherwise minimal impact on the model chemistry. Observed MHP concentrations in the dry free troposphere are much less sensitive to MD interference and vary with the branching ratio of the CH_3O_2 reaction with HO_2 versus NO, supporting current understanding of low-NO and high-NO chemical regimes for VOC oxidation.

Plain Language Summary Methyl hydroperoxide (MHP) is a chemical compound commonly found in clean, remote regions of the atmosphere. However, aircraft measurements over Seoul, South Korea, have reported unexpectedly high levels of MHP in the city's polluted air. The instrument used to measure MHP also detects an isomer called methanediol, with higher sensitivity especially under humid conditions. Methanediol has recently gained attention as a possible key ingredient in the formation of formic acid, but very few observations are available. We find that including methanediol chemistry in the GEOS-Chem atmospheric chemistry model increases the global formic acid source by 11% and has a negligible effect on other chemical species. At higher altitudes, where the air is drier, the methanediol impact on MHP observations is small. Under these conditions, reported MHP concentrations are consistent with model simulations.

Key Points:

- Aircraft observations of methyl hydroperoxide (MHP) over Seoul are 4× higher than in the GEOS-Chem model, likely due to methanediol interference
- Free tropospheric MHP is consistent with oxidation of methane over a range of HO_2/NO concentration ratios
- Adding in-cloud formaldehyde hydration as a source of methanediol in the GEOS-Chem increases the global formic acid source by 11%

Supporting Information:

Supporting Information may be found in the online version of this article.

Correspondence to:

L. H. Yang,
laurayang@g.harvard.edu

Citation:

Yang, L. H., Jacob, D. J., Bates, K. H., Lin, H., Allen, H. M., Müller, J.-F., et al. (2025). Modeling of methyl hydroperoxide observations in urban and remote air over South Korea: Methylperoxy radical chemistry and inference of atmospheric methanediol. *Geophysical Research Letters*, *52*, e2025GL118267. https://doi.org/10.1029/2025GL118267

Received 22 JUL 2025
Accepted 3 OCT 2025

Author Contributions:

Conceptualization: L. H. Yang, D. J. Jacob
Formal analysis: L. H. Yang
Funding acquisition: D. J. Jacob, K. Li, H. Liao
Investigation: L. H. Yang
Methodology: L. H. Yang, K. H. Bates, H. Lin, H. M. Allen, S. Zhai, J. D. Crounse
Resources: J. F. Brewer
Software: R. M. Yantosca
Supervision: D. J. Jacob

1. Introduction

Methyl hydroperoxide (CH_3OOH, MHP) is produced in the atmospheric oxidation of methane and higher volatile organic compounds (VOCs) under clean conditions with low concentrations of nitrogen oxides ($NO_x \equiv NO + NO_2$). Observations from the KORUS-AQ aircraft campaign (Crawford et al., 2021) over South Korea report four times higher MHP concentrations than chemical transport model (CTM) simulations, and here we investigate why.

Validation: H. Lin, H. M. Allen, J.-F. Müller, R. Dang, N. K. Colombi, N. L. Ng, J. D. Crounse, P. O. Wennberg
Visualization: L. H. Yang, J.-F. Müller
Writing – original draft: L. H. Yang
Writing – review & editing: L. H. Yang, D. J. Jacob, K. H. Bates, H. Lin, H. M. Allen, J.-F. Müller, S. S. Brown, R. Dang, N. K. Colombi, S. Zhai, R. M. Yantosca, J. F. Brewer, N. L. Ng, J. D. Crounse, P. O. Wennberg, K. Li, H. Liao

The only known atmospheric source of MHP is the reaction of the methylperoxy radical (CH_3O_2) with the hydroperoxyl radical (HO_2) (T. L. Nguyen & Stanton, 2022):

$$CH_3O_2 + HO_2 \rightarrow CH_3OOH + O_2 \quad (1)$$

CH_3O_2 is the first-generation product from the atmospheric oxidation of methane by the hydroxyl radical (OH). It is also a later-generation product from the atmospheric oxidation cascade of non-methane VOCs. HO_2 is an ubiquitous radical that cycles with OH, originating primarily from the photo-oxidation of water by $H_2O + O(^1D)$. Reaction 1 competes with the reaction of CH_3O_2 with nitric oxide (NO):

$$CH_3O_2 + NO \xrightarrow{+O_2} CH_2O + NO_2 + HO_2 \quad (2)$$

Because of this competition, MHP concentrations are expected to be low in polluted environments with high NO_x emissions from fuel combustion. Competition between Reactions 1 and 2 for CH_3O_2 and other peroxy radicals controls tropospheric ozone (O_3) and secondary organic aerosol production from VOC oxidation.

Loss of MHP is by reaction with OH (typically ~80%) and photolysis (~20%), with an average lifetime of a few days (T. L. Nguyen et al., 2022; Snow et al., 2007). MHP is a major contributor to total OH reactivity in clean air (Travis et al., 2020), and as such, it affects the lifetimes of all gases oxidized by OH. It is sparingly soluble in water and therefore not efficiently removed by wet or dry deposition. Deep convection injects MHP into the upper troposphere (Snow et al., 2007) where subsequent photolysis is a source of OH (Jaeglé et al., 1997).

Atmospheric observations of MHP have received relatively little attention from a chemical modeling perspective. Field studies show concentrations of 0.1–1 ppb in surface air (Moortgat et al., 2002; Watanabe et al., 2017; X. Zhang et al., 2012), highest in summer (Klippel et al., 2011; Morgan & Jackson, 2002; Q. Zhang et al., 2018; X. Zhang et al., 2012). Aircraft observations in the continental planetary boundary layer (PBL) typically extending to ~2 km indicate values higher than in surface air (Klippel et al., 2011; Weinstein-Lloyd et al., 1998; J. Zheng et al., 2002), as might be expected from lower NO concentrations. MHP concentrations generally drop in the free troposphere (FT) above the PBL due to low water vapor and because cold temperatures suppress the oxidation of methane, but high values can be observed as a result of deep convection (Allen, Bates, et al., 2022; Jaeglé et al., 1997; Ravetta et al., 2001; Snow et al., 2003).

The KORUS-AQ aircraft campaign over the Seoul Metropolitan Area (SMA) and the Korean Peninsula in May–June 2016 characterized atmospheric chemistry in the polluted PBL and the background FT (Crawford et al., 2021). MHP was measured with a CF_3O^- California Institute of Technology Chemical Ionization Mass Spectrometer (CIT-CIMS, Allen, Crounse, et al., 2022). Reported PBL concentrations over the SMA were in the range 0.5–1.5 ppb, which is remarkably high for such a polluted environment. For instance, in Beijing, surface MHP concentrations are 0.1–0.2 ppb (X. Zhang et al., 2012).

Positive interference in the CIT-CIMS MHP measurement is expected from methanediol ($CH_2(OH)_2$, MD), which has the same molecular weight. MD is produced from the hydration of formaldehyde (CH_2O) in clouds (Jacob, 1986) and is of interest as an atmospheric source of formic acid (HCOOH, Franco et al., 2021; T. L. Nguyen et al., 2023). But there have been no direct observations of MD concentrations. Gao et al. (2022) inferred an upper limit of 20 ppt from CIMS measurements at a rural site in summer. Allen, Crounse, et al. (2022) inferred an upper limit of 12 ppt from CIT-CIMS in marine air during the ATom aircraft campaign. Global MAGRITTE model values reported by T. L. Nguyen et al. (2023) are in the range 1–50 ppt, mostly tracking CH_2O. These values are much lower than typical MHP concentrations, but the CIT-CIMS sensitivity to MHP declines at high water vapor and temperature, and this could make MD observable.

Here we interpret the KORUS-AQ observations of MHP (+MD) in the PBL and the FT using the GEOS-Chem CTM with detailed atmospheric chemistry. Yang et al. (2023) previously showed that GEOS-Chem successfully simulates observed concentrations of oxidants and related species in KORUS-AQ, including ozone, NO_x, OH, and HO_2. However, the model underestimates reported MHP in the PBL by a factor of 4. We show that 70% of this underestimate can be accounted for by including MD chemistry in GEOS-Chem. We further show that the reported MHP in the FT supports current understanding of CH_3O_2 chemistry and the competition between Reactions 1 and 2 that defines the low-NO and high-NO regimes for VOC oxidation.

2. Methods

2.1. GEOS-Chem Model

We use GEOS-Chem version 13.3.4 (https://doi.org/10.5281/zenodo.5764874), driven by NASA Goddard Earth Observing System—Forward Processing (GEOS-FP) assimilated meteorological data, at 0.25° × 0.3125° horizontal resolution over South Korea (29°N–40°N, 120°E–135°E) with 29 vertical levels in the troposphere and nested within a global simulation at 4° × 5° resolution providing dynamic boundary conditions updated every 3 hr. We initialize the model for 6 months and conduct the simulation for April–June 2016. Anthropogenic emissions include the Multi-resolution Emission Inventory for China (MEIC, B. Zheng et al., 2018), the KORUSv5 inventory (Woo et al., 2020) for the rest of Asia, and the Community Emissions Data System (CEDSv2, McDuffie et al., 2021) outside of Asia. Natural emissions include MEGANv2 (Guenther et al., 2012) for biogenic NMVOCs, Hudman et al. (2012) for soil NO_x, and Murray et al. (2012) for lightning NO_x.

GEOS-Chem version 13.3.4 includes 293 species and 902 reactions to describe oxidant-aerosol tropospheric chemistry. Following Yang et al. (2023), we modify the mechanism to add aerosol nitrate photolysis (Choi et al., 2019; Shah et al., 2024), volatile chemical product emissions and chemistry (Coggon et al., 2021), coarse anthropogenic dust uptake of HNO_3 (Zhai et al., 2023), and reduce the HO_2 reactive uptake coefficient by aerosols from 0.2 to 0.1 (Yang et al., 2023). Yang et al. (2023) showed that the GEOS-Chem version 13.3.4 with these modifications could better simulate ozone and HO_x concentrations during KORUS-AQ. Aerosol nitrate photolysis, the most important factor, was added in the standard GEOS-Chem version 14.2.0.

Here we add MD to the GEOS-Chem mechanism following the pathways and kinetics described by T. L. Nguyen et al. (2023). MD is a gem-diol formed by aqueous phase CH_2O hydration in clouds. It is released to the gas phase upon cloud evaporation, and its dominant sinks are oxidation by OH (averaging 60% globally) to produce formic acid and dry and wet deposition (40%), resulting in a global mean tropospheric lifetime of 2 days. Franco et al. (2021) proposed that oxidation of MD could be a major atmospheric source of formic acid, but T. L. Nguyen et al. (2023) found the oxidation of MD by OH to be three times lower than estimated by Franco et al. (2021), allowing MD deposition to compete with OH oxidation, and greatly reducing the source of formic acid.

We follow the parameterization of T. L. Nguyen et al. (2023) for the model representation of their MD mechanism. That parameterization computes a first-order rate constant for net conversion of CH_2O to MD in the gas phase on the basis of cloud fraction, liquid water content (LWC), temperature, and in-cloud residence time. Cloud fraction, LWC, and temperature are taken here from the GEOS-FP meteorological fields used to drive GEOS-Chem (Figure S1 in Supporting Information S1), and in-cloud residence time is assumed to be 1 hr. Figure S2 in Supporting Information S1 shows the sensitivity results for different in-cloud residence times.

Figure 1 shows the global distributions of simulated surface MHP, MD, and CH_2O concentrations in GEOS-Chem for the KORUS-AQ period. MHP concentration is highest over tropical continents due to high biogenic VOC emissions and low NO concentrations. MD concentrations are generally higher over land, following CH_2O, but are shifted toward higher latitudes and altitudes than CH_2O, reflecting cloud processing. Surface MD concentrations are of the order of 10 ppt, consistent with the range and patterns obtained by T. L. Nguyen et al. (2023) with the MAGRITTE model. MD formation in GEOS-Chem decreases CH_2O levels by less than 1% because photolysis and oxidation by OH are much faster CH_2O sinks, and it has negligible effects on other aspects of oxidant chemistry. It slightly increases the chemical source of formic acid, and that will be discussed below.

2.2. KORUS-AQ Observations

Twenty research flights were conducted between 08:00 and 16:00 local time during the KORUS-AQ campaign with the NASA-DC8 aircraft. The flights covered the Korean Peninsula with the highest density of observations in the SMA. The aircraft carried an extensive payload, including measurements of MHP, H_2O_2, VOCs, NO, HO_2, and OH concentrations, among others. We use a 60-s merged data set (https://www-air.larc.nasa.gov/, last accessed: 15 July 2025). Observations of the Daesan power plant plume (36.4°N–37.15°N, 126°E–126.88°E) are excluded from analysis. The aircraft avoided clouds, and the MHP data exclude water vapor concentrations greater than 1×10^4 ppm, so we consider the measurements to be representative of the gas phase.

The CIT-CIMS measurements are reported as MHP but actually represent the sum of MHP and MD concentrations weighted by their relative sensitivities to water vapor interference (Allen, Crounse, et al., 2022; Crounse

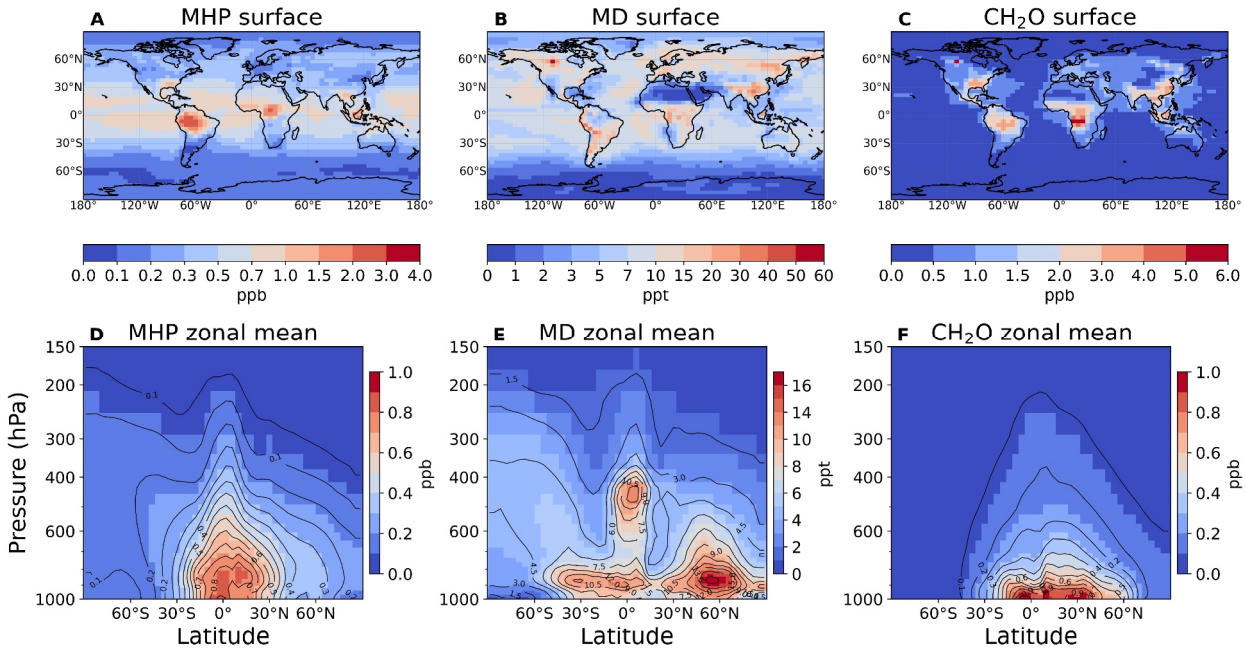

Figure 1. Global distributions of methyl hydroperoxide (MHP), methanediol (MD), and formaldehyde (CH_2O) concentrations in GEOS-Chem. Values are May–June 2016 means from a global simulation with 4° × 5° resolution. The top row shows surface concentrations and the bottom row shows zonal mean concentrations as a function of latitude and pressure. Note the different scales for the different panels. The hotspot of MD and CH_2O over Canada is due to a wildfire.

et al., 2006). The lack of a precise and stable standard of MD limits accurate calibration of its relative sensitivity, defined as how the signal changes relative to the value when there is negligible water interference. The relative sensitivity of MD has been assumed to follow the hydroxymethyl hydroperoxide (HMHP) calibration curve by chemical analogy (Allen, Crounse, et al., 2022; T. B. Nguyen et al., 2016). HMHP, unlike MHP, shows no reduction in relative sensitivity with water vapor. Figure 2a shows the calibration curves for MD ($S_{MD,1}$) and MHP ($S_{MHP,1}$), without dilution. The CIT-CIMS dilutes ambient air with N_2 by a factor of 5 ± 3 before ionization to reduce complications arising from high water vapor levels within the instrument (Allen, Crounse, et al., 2022; St. Clair et al., 2010) and improve the relative sensitivity to MHP. The dilution factor typically varies by as much as 40% throughout a flight as a function of instrument temperature.

As shown in the next section, the calibration curves with dilution factors cannot reconcile the observed MHP concentrations with the sum of modeled MHP and MD concentrations. The modeled concentrations are consistent with the observations only when the assumed dilution factor is on the order of 1, that is, much lower than the

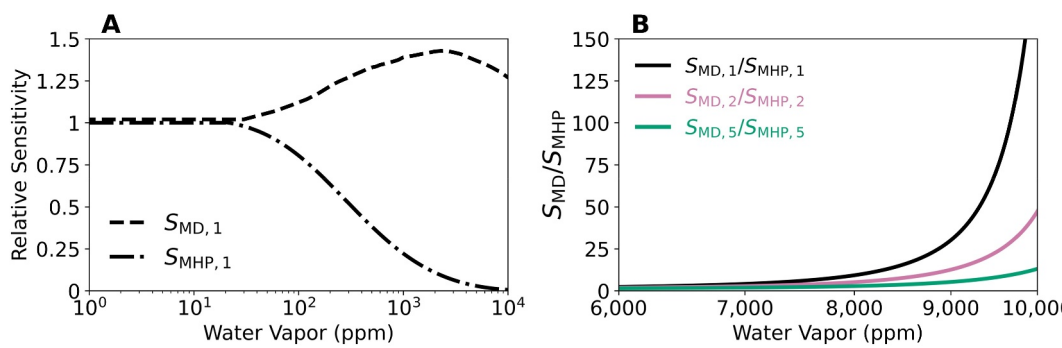

Figure 2. (a) Relative sensitivity S of the CF_3O^- CIT-CIMS instrument to methyl hydroperoxide (MHP) and methanediol (MD), versus ambient water vapor concentrations. The relative sensitivity of MD (S_{MD}) is assumed to be the same as for hydromethyl hydroperoxide (HMHP). $S_{MHP,1}$ and $S_{MD,1}$ are taken from Allen, Crounse, et al. (2022) without air dilution in the instrument. (b) Ratio of relative sensitivities between MD and MHP (S_{MD}/S_{MHP}) under different assumed dilution factors. $S_{MD,1}/S_{MHP,1}$, $S_{MD,2}/S_{MHP,2}$, and $S_{MD,5}/S_{MHP,5}$ correspond to dilution factors of 1, 2, and 5, respectively.

expected range during the campaign (5 ± 3). This discrepancy may be related to remaining uncertainties in (a) the effective dilution factor, (b) the calibration curve at high water vapor concentrations, (c) a potential underestimate of cloudiness or LWC in the model, (d) the cloud residence time (Figure S2 in Supporting Information S1), (e) an underestimate of $[CH_2O]$ in the model, and (f) the assumed analogy between MD and HMHP sensitivities.

The CIT-CIMS detects $S_{MHP}[MHP] + S_{MD}[MD]$, but only the S_{MHP} correction is applied before reporting the data as [MHP], ignoring the contribution from MD. To estimate this contribution in GEOS-Chem, we scale simulated [MD] by $S_{MD,x}/S_{MHP,x}$ where x represents the dilution factor:

$$[\mathbf{MD}]_x^* = \frac{\boldsymbol{S_{MD,x}}}{\boldsymbol{S_{MHP,x}}}[\mathbf{MD}] \quad (3)$$

Reported [MHP] can then be compared to the model $[MHP] + [MD]_x^*$.

Figure 2b shows the ranges of $S_{MD,x}/S_{MHP,x}$ for dilution factors 1, 2 (St. Clair et al., 2010), and 5 (Allen, Crounse, et al., 2022), representing the plausible ranges of the calibration curves to account for uncertainties in both the dilution factor and the relative sensitivity of MD. Despite [MD]/[MHP] $\sim 10^{-2}$ in GEOS-Chem, the $[MD]^*$ correction can be important in the PBL where water vapor concentrations are high (Figure 2b). At water vapor concentrations of 1×10^4 ppm, the instrument is 10 times more sensitive to MD than MHP when using a dilution factor of 5, 50 times more sensitive when using a dilution factor of 2, and 150 times more sensitive when assuming no dilution.

3. Results and Discussion

Figure 3 shows the median vertical concentration profiles of HO_2, NO, MHP, CH_2O, and water vapor over the SMA during the KORUS-AQ campaign. The same figure for the whole of the KORUS-AQ campaign is shown in Figure S3 in Supporting Information S1. Aircraft observations are compared to GEOS-Chem model values sampled along the flight tracks. HO_2 and NO compete for CH_3O_2 via Reactions 1 and 2, forming MHP in the former, while CH_2O is ultimately produced by both pathways. From measured and modeled HO_2 and NO concentrations, we derive the branching ratio f_{HO_2} also shown in Figure 3:

$$f_{HO_2} = \frac{k_{CH_3O_2+HO_2}[HO_2]}{k_{CH_3O_2+NO}[NO] + k_{CH_3O_2+HO_2}[HO_2]} \quad (4)$$

where the rate coefficients k are from Burkholder et al. (2020). f_{HO_2} represents the MHP yield from CH_3O_2 radicals. Additional CH_3O_2 sinks from reactions with other organic peroxy radicals and with NO_2 contribute less than 10% to the total sink under all KORUS-AQ conditions.

Observed HO_2 concentrations in Figure 3 increase from 2 ppt near the surface to 18 ppt in the FT, consistent with GEOS-Chem, where this increase is due to lower NO concentrations in the FT. The NO concentration decreases from 7 ppb near the surface to 0.04 ppb in the FT. The resulting f_{HO_2} increases from near-zero near the surface to 0.3 in the FT, higher in the observations than in the model because of higher NO in the model. The median MHP in the observations is 0.81 ppb in the PBL and 0.29 ppb in the FT. The corresponding model values are 0.21 ppb in the PBL and 0.17 ppb in the FT, underestimating observations by a factor of 4 in the PBL and a factor of 2 in the FT.

The low MHP concentration in GEOS-Chem in the PBL reflects the low f_{HO_2}, and the observations show similarly low f_{HO_2}. The PBL source of CH_3O_2 in GEOS-Chem is mainly from the oxidation of non-methane VOCs (Kim et al., 2022). The CH_2O concentration is underestimated by 40% due to missing VOCs (Beaudry et al., 2025; Travis et al., 2024), implying a corresponding underestimate in the CH_3O_2 source, but this would not resolve the discrepancy with the reported MHP. Median GEOS-Chem concentrations of MD in the SMA during KORUS-AQ are 5 ppt in surface air, 5–6 ppt in the PBL, and 2–3 ppt in the FT, where the decrease with altitude tracks CH_2O. The near-surface MD concentration for June over Seoul is 13 ppt in the global model calculations of T. L. Nguyen et al. (2023). GEOS-Chem MD concentration is a factor of 2–3 lower, which may be due to a difference in cloud fields.

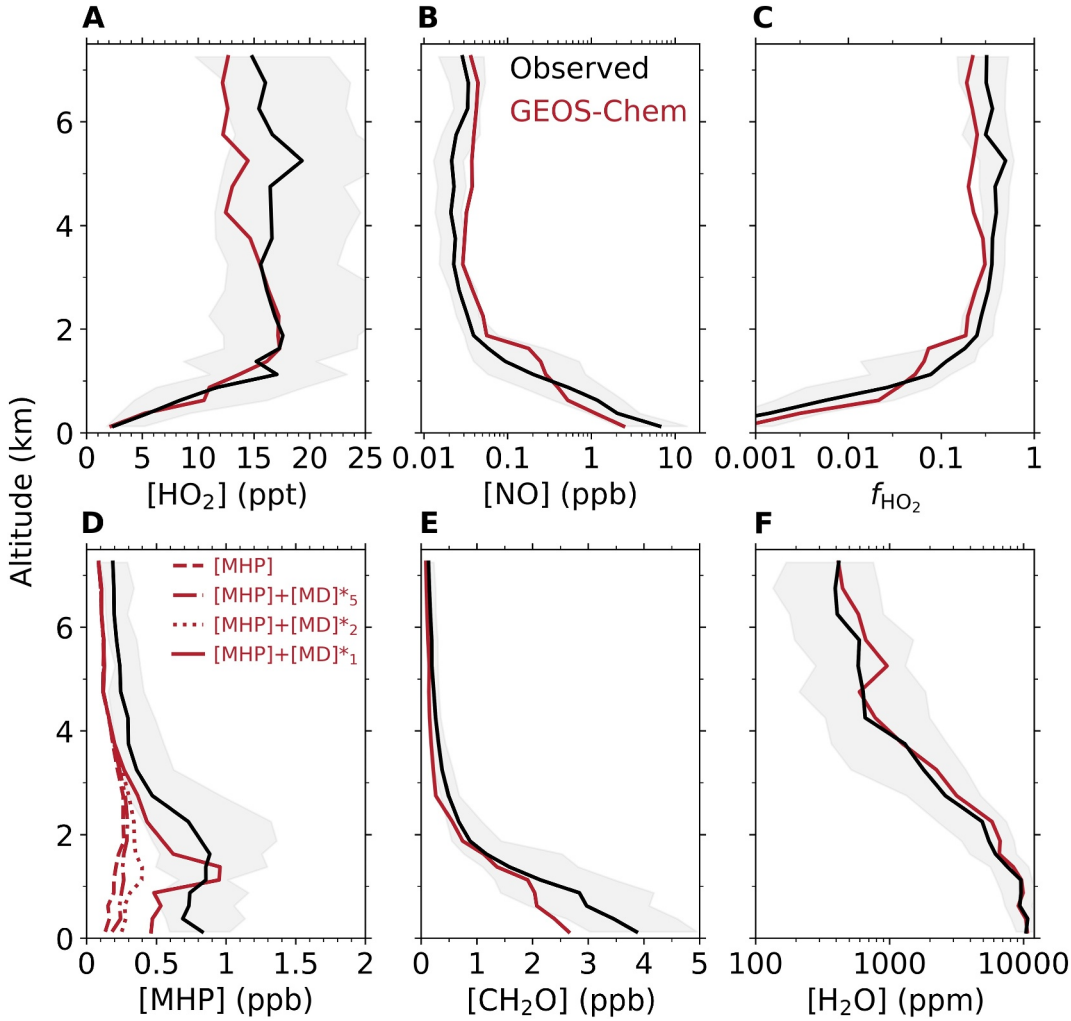

Figure 3. Median vertical profiles of species concentrations and of the CH_3O_2 branching ratio f_{HO_2} (Equation 4) over the Seoul Metropolitan Area (37°N–37.6°N, 126.6°E–127.7°E) during the KORUS-AQ aircraft campaign (May–June 2016). Note the log scales for NO, f_{HO_2}, and H_2O. Observations (with interquartile in shading) are compared to the GEOS-Chem model sampled along the aircraft flight tracks. The methyl hydroperoxide (MHP) data exclude water vapor concentrations greater than 1×10^4 ppm (37% of data below 2 km altitude), which lie beyond the range of the calibration curves in Figure 2. [MHP] + $[MD]^*_x$ where x is the dilution factor includes model methanediol with correction for MHP relative sensitivity as given by Equation 3.

Adding $[MD]^*_x$ as defined in Equation 3 to the simulated MHP concentrations in the PBL increases the concentration by only 30%–50% when using $[MD]^*_5$, 60%–90% when using $[MD]^*_2$, but by a factor of 3 when using $[MD]^*_1$. Addition of $[MD]^*_1$ largely corrects the model to match the magnitude of the observations (base run hereafter), though a 30%–50% discrepancy remains that might be explained by the CH_2O underestimate. The model now shows a maximum at 1.4 km altitude reflecting cloud processing; the observations also show a maximum in this altitude range, though it is broader. The MHP discrepancy between model and observations could thus possibly be resolved by a contribution of MD to the observations, though major uncertainties remain in the model MD concentrations and the instrument calibration curve.

The MHP model underestimate extends into the FT, where production should mainly be from the oxidation of methane, and where the $[MD]^*$ correction is, in general, small because the air is dry. Figure 4 shows the observed and modeled dependences of MHP concentrations on the branching ratio f_{HO_2} (Equation 4), including linear regressions for background FT conditions with $[H_2O] < 700$ ppm. Under these background conditions, we find that the MHP concentration is successfully predicted from f_{HO_2} in both the model and observations, with

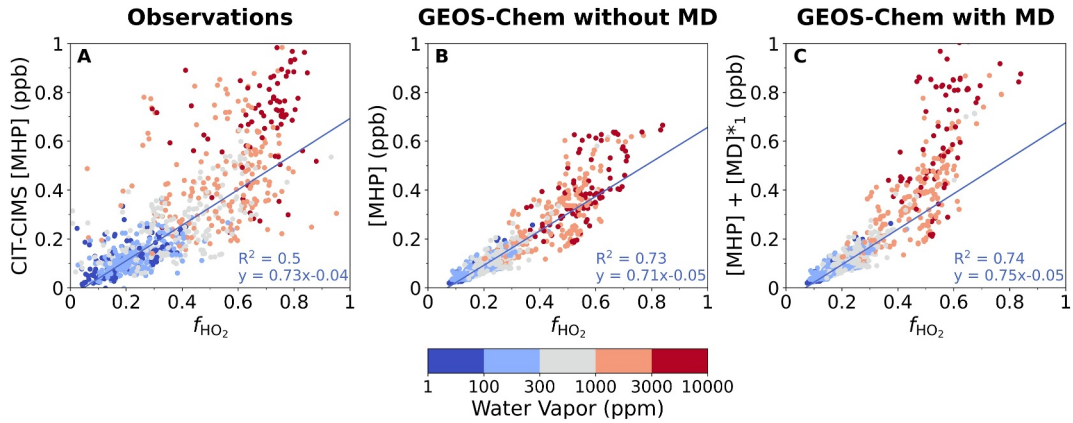

Figure 4. Relationship of methyl hydroperoxide (MHP) with the fraction of CH_3O_2 reacting with HO_2 (f_{HO_2}, Equation 4) in the free troposphere (>4 km altitude) during KORUS-AQ. Panel (a) shows the relationship in the observations and panel (b) shows the relationship in the model. Panel (c) adds $[MD]_1^*$ to the MHP concentration in the model. Data points are colored by water vapor concentrations (ppm). The coefficient of determination (R^2) and the reduced-major axis linear regression are shown for data with water vapor concentrations <700 ppm.

consistent slopes. The relationship breaks down at high water vapor mixing ratio in both the model and observations, reflecting recent convective injection of PBL air. The effect is much larger in the observations, as might be expected given the model underestimate in the PBL. Accounting for $[MD]_1^*$ in the model captures the observed enhancements in recently convected air while not affecting the fit to f_{HO_2} under background conditions (Figure 4c). The model underestimate of median MHP concentrations in the FT can be simply explained by an underestimate of f_{HO_2} resulting from excessive NO (Figure 3). Our analysis of the FT data thus confirms the general mechanism for MHP production as driven by the CH_3O_2 + HO_2 reaction competing with the CH_3O_2 + NO reaction, with current knowledge of kinetics, and with CH_3O_2 in the FT originating mainly from the oxidation of methane.

The most important consequence of MD chemistry in GEOS-Chem is for formic acid formation. We find in GEOS-Chem a global formic acid source from MD + OH of 4.1 Tg a^{-1}, consistent with 1.2–8.5 Tg a^{-1} from T. L. Nguyen et al. (2023) but smaller than other atmospheric sources, including glycoaldehyde + OH (19.5 Tg a^{-1}) and hydrolysis of Criegee Intermediate produced from ozonolysis of terminal alkenes (7.6 Tg a^{-1}). The global chemical source of formic acid in GEOS-Chem is 44 Tg a^{-1}, smaller than the global source of 100–120 Tg a^{-1} needed to explain atmospheric observations (Stavrakou et al., 2012). The nature of the missing source remains unclear.

In summary, the four-fold GEOS-Chem model underestimate of MHP concentrations measured in the PBL of the SMA during the KORUS-AQ aircraft campaign may be explained at least in part by positive interference in the measurements from methanediol (MD) produced by the hydration of formaldehyde in clouds. Including MD chemistry in GEOS-Chem increases the global model source of formic acid by 11% but has no other significant chemical effects. By contrast, observed MHP concentrations and their variability in the background FT (above 4 km altitude) during KORUS-AQ align closely with our fundamental understanding of MHP formation determined by competition between the CH_3O_2 + HO_2 and CH_3O_2 + NO reactions, where both HO_2 and NO concentrations were measured in KORUS-AQ, and where CH_3O_2 originates mainly from the oxidation of methane. This confirms current understanding of high-NO and low-NO pathways for the oxidation cascade of VOCs driving ozone and organic aerosol formation.

Conflict of Interest

The authors declare no conflicts of interest relevant to this study.

Data Availability Statement

The KORUS-AQ data archive is available at https://doi.org/10.5067/Suborbital/KORUSAQ/DATA01 (NASA, 2019). The ATom data archive is available at https://doi.org/10.3334/ORNLDAAC/1581 (Wofsy et al., 2018). The model code used in this work is available at https://doi.org/10.5281/zenodo.5764874 (The International GEOS-Chem User Community, 2021).

Acknowledgments
The authors would like to acknowledge KORUS-AQ data provides including William H. Brune for ATHOS and Alan Fried for CAMS measurements. We thank Jim Crawford and Katherine R. Travis for helpful discussions. This material is based upon work supported by the National Science Foundation Graduate Research Fellowship under Grant DGE 2140743, the Harvard–NUIST Joint Laboratory for Air Quality and Climate, and the NASA Atmospheric Composition Campaign Data Analysis and Modeling (ACCDAM) Program.

References

Allen, H. M., Bates, K. H., Crounse, J. D., Kim, M. J., Teng, A. P., Ray, E. A., & Wennberg, P. O. (2022). H_2O_2 and CH_3OOH (MHP) in the remote atmosphere: 2. Physical and chemical controls. *Journal of Geophysical Research: Atmospheres*, *127*(6), e2021JD035702. https://doi.org/10.1029/2021JD035702

Allen, H. M., Crounse, J. D., Kim, M. J., Teng, A. P., Ray, E. A., McKain, K., et al. (2022). H_2O_2 and CH_3OOH (MHP) in the remote atmosphere: 1. Global distribution and regional influences. *Journal of Geophysical Research: Atmospheres*, *127*(6), e2021JD035701. https://doi.org/10.1029/2021JD035701

Beaudry, E., Jacob, D. J., Bates, K. H., Zhai, S., Yang, L. H., Pendergrass, D. C., et al. (2025). Ethanol and methanol in South Korea and China: Evidence for large anthropogenic emissions missing from current inventories. *ACS ES&T Air*, *2*(4), 456–465. https://doi.org/10.1021/acsestair.4c00210

Burkholder, J. B., Sander, S. P., Abbatt, J. P. D., Barker, J. R., Cappa, C., Crounse, J. D., & Dibble, T. S. (2020). *JPL publication 19-5. Chemical kinetics and photochemical data for use in atmospheric studies*. NASA Jet Propulsion Laboratory. Retrieved from https://hdl.handle.net/2014/49199

Choi, J., Park, R. J., Lee, H.-M., Lee, S., Jo, D. S., Jeong, J. I., et al. (2019). Impacts of local vs. trans-boundary emissions from different sectors on $PM_{2.5}$ exposure in South Korea during the KORUS-AQ campaign. *Atmospheric Environment*, *203*, 196–205. https://doi.org/10.1016/j.atmosenv.2019.02.008

Coggon, M. M., Gkatzelis, G. I., McDonald, B. C., Gilman, J. B., Schwantes, R. H., Abuhassan, N., et al. (2021). Volatile chemical product emissions enhance ozone and modulate urban chemistry. *Proceedings of the National Academy of Sciences of the United States of America*, *118*(32), e2026653118. https://doi.org/10.1073/pnas.2026653118

Crawford, J. H., Ahn, J.-Y., Al-Saadi, J., Chang, L., Emmons, L. K., Kim, J., et al. (2021). The Korea–United States air quality (KORUS-AQ) field study. *Elementa: Science of the Anthropocene*, *9*(1), 00163. https://doi.org/10.1525/elementa.2020.00163

Crounse, J. D., McKinney, K. A., Kwan, A. J., & Wennberg, P. O. (2006). Measurement of gas-phase hydroperoxides by chemical ionization mass spectrometry. *Analytical Chemistry*, *78*(19), 6726–6732. https://doi.org/10.1021/ac0604235

Franco, B., Blumenstock, T., Cho, C., Clarisse, L., Clerbaux, C., Coheur, P.-F., et al. (2021). Ubiquitous atmospheric production of organic acids mediated by cloud droplets. *Nature*, *593*(7858), 233–237. https://doi.org/10.1038/s41586-021-03462-x

Gao, Z., Vasilakos, P., Nah, T., Takeuchi, M., Chen, H., Tanner, D. J., et al. (2022). Emissions, chemistry or bidirectional surface transfer? Gas phase formic acid dynamics in the atmosphere. *Atmospheric Environment*, *274*, 118995. https://doi.org/10.1016/j.atmosenv.2022.118995

Guenther, A. B., Jiang, X., Heald, C. L., Sakulyanontvittaya, T., Duhl, T., Emmons, L. K., & Wang, X. (2012). The model of emissions of gases and aerosols from nature version 2.1 (MEGAN2.1): An extended and updated framework for modeling biogenic emissions. *Geoscientific Model Development*, *5*(6), 1471–1492. https://doi.org/10.5194/gmd-5-1471-2012

Hudman, R. C., Moore, N. E., Mebust, A. K., Martin, R. V., Russell, A. R., Valin, L. C., & Cohen, R. C. (2012). Steps towards a mechanistic model of global soil nitric oxide emissions: Implementation and space based-constraints. *Atmospheric Chemistry and Physics*, *12*(16), 7779–7795. https://doi.org/10.5194/acp-12-7779-2012

The International GEOS-Chem User Community. (2021). geoschem/GC-Classic: GEOS-chem 13.3.4 (13.3.4) [Software]. *Zenodo*. https://doi.org/10.5281/zenodo.5764874

Jacob, D. J. (1986). Chemistry of OH in remote clouds and its role in the production of formic acid and peroxymonosulfate. *Journal of Geophysical Research*, *91*(D9), 9807–9826. https://doi.org/10.1029/JD091iD09p09807

Jaeglé, L., Jacob, D. J., Wennberg, P. O., Spivakovsky, C. M., Hanisco, T. F., Lanzendorf, E. J., et al. (1997). Observed OH and HO_2 in the upper troposphere suggest a major source from convective injection of peroxides. *Geophysical Research Letters*, *24*(24), 3181–3184. https://doi.org/10.1029/97GL03004

Kim, H., Park, R. J., Kim, S., Brune, W. H., Diskin, G. S., Fried, A., et al. (2022). Observed versus simulated OH reactivity during KORUS-AQ campaign: Implications for emission inventory and chemical environment in East Asia. *Elementa: Science of the Anthropocene*, *10*(1), 00030. https://doi.org/10.1525/elementa.2022.00030

Klippel, T., Fischer, H., Bozem, H., Lawrence, M. G., Butler, T., Jöckel, P., et al. (2011). Distribution of hydrogen peroxide and formaldehyde over Central Europe during the HOOVER project. *Atmospheric Chemistry and Physics*, *11*(9), 4391–4410. https://doi.org/10.5194/acp-11-4391-2011

McDuffie, E. E., Martin, R. V., Spadaro, J. V., Burnett, R., Smith, S. J., O'Rourke, P., et al. (2021). Source sector and fuel contributions to ambient $PM_{2.5}$ and attributable mortality across multiple spatial scales. *Nature Communications*, *12*(1), 3594. https://doi.org/10.1038/s41467-021-23853-y

Moortgat, G. K., Grossmann, D., Boddenberg, A., Dallmann, G., Ligon, A. P., Turner, W. V., et al. (2002). Hydrogen peroxide, organic peroxides and higher carbonyl compounds determined during the BERLIOZ campaign. In W. Seiler, K.-H. Becker, & E. Schaller (Eds.), *Tropospheric chemistry* (pp. 443–463). Springer Netherlands. https://doi.org/10.1007/978-94-010-0399-5_18

Morgan, R. B., & Jackson, A. V. (2002). Measurements of gas-phase hydrogen peroxide and methyl hydroperoxide in the coastal environment during the PARFORCE project. *Journal of Geophysical Research*, *107*(D19), PAR13-1–PAR13-9. https://doi.org/10.1029/2000JD000257

Murray, L. T., Jacob, D. J., Logan, J. A., Hudman, R. C., & Koshak, W. J. (2012). Optimized regional and interannual variability of lightning in a global chemical transport model constrained by LIS/OTD satellite data. *Journal of Geophysical Research*, *117*(D20), 2012JD017934. https://doi.org/10.1029/2012JD017934

NASA. (2019). KORUS-AQ: Korea United States air quality study [Dataset]. *Atmospheric Science Data Center*. https://doi.org/10.5067/Suborbital/KORUSAQ/DATA01

Nguyen, T. B., Tyndall, G. S., Crounse, J. D., Teng, A. P., Bates, K. H., Schwantes, R. H., et al. (2016). Atmospheric fates of Criegee intermediates in the ozonolysis of isoprene. *Physical Chemistry Chemical Physics*, *18*(15), 10241–10254. https://doi.org/10.1039/c6cp00053c

Nguyen, T. L., Peeters, J., Müller, J.-F., Perera, A., Bross, D. H., Ruscic, B., & Stanton, J. F. (2023). Methanediol from cloud-processed formaldehyde is only a minor source of atmospheric formic acid. *Proceedings of the National Academy of Sciences of the United States of America*, *120*(48), e2304650120. https://doi.org/10.1073/pnas.2304650120

Nguyen, T. L., Perera, A., & Peeters, J. (2022). High-accuracy first-principles-based rate coefficients for the reaction of OH and CH_3OOH. *Physical Chemistry Chemical Physics*, *24*(43), 26684–26691. https://doi.org/10.1039/D2CP03919B

Nguyen, T. L., & Stanton, J. F. (2022). The reaction of HO_2 and CH_3O_2: CH_3OOH formed from the singlet electronic state surface. *Atmosphere*, *13*(9), 1397. https://doi.org/10.3390/atmos13091397

Ravetta, F., Jacob, D. J., Brune, W. H., Heikes, B. G., Anderson, B. E., Blake, D. R., et al. (2001). Experimental evidence for the importance of convected methylhydroperoxide as a source of hydrogen oxide (HOx) radicals in the tropical upper troposphere. *Journal of Geophysical Research*, *106*(D23), 32709–32716. https://doi.org/10.1029/2001JD900009

Shah, V., Keller, C. A., Knowland, K. E., Christiansen, A., Hu, L., Wang, H., et al. (2024). Particulate nitrate photolysis as a possible driver of rising tropospheric ozone. *Geophysical Research Letters*, *51*(5), e2023GL107980. https://doi.org/10.1029/2023GL107980

Snow, J. A., Heikes, B. G., Merrill, J. T., Wimmers, A. J., Moody, J. L., & Cantrell, C. A. (2003). Winter-spring evolution and variability of HOx reservoir species, hydrogen peroxide, and methyl hydroperoxide, in the northern middle to high latitudes. *Journal of Geophysical Research*, *108*(D4), 2002JD002172. https://doi.org/10.1029/2002JD002172

Snow, J. A., Heikes, B. G., Shen, H., O'Sullivan, D. W., Fried, A., & Walega, J. (2007). Hydrogen peroxide, methyl hydroperoxide, and formaldehyde over North America and the North Atlantic. *Journal of Geophysical Research*, *112*(D12), 2006JD007746. https://doi.org/10.1029/2006JD007746

Stavrakou, T., Müller, J.-F., Peeters, J., Razavi, A., Clarisse, L., Clerbaux, C., et al. (2012). Satellite evidence for a large source of formic acid from boreal and tropical forests. *Nature Geoscience*, *5*(1), 26–30. https://doi.org/10.1038/ngeo1354

St. Clair, J. M., McCabe, D. C., Crounse, J. D., Steiner, U., & Wennberg, P. O. (2010). Chemical ionization tandem mass spectrometer for the in situ measurement of methyl hydrogen peroxide. *Review of Scientific Instruments*, *81*(9), 094102. https://doi.org/10.1063/1.3480552

Travis, K. R., Heald, C. L., Allen, H. M., Apel, E. C., Arnold, S. R., Blake, D. R., et al. (2020). Constraining remote oxidation capacity with ATom observations. *Atmospheric Chemistry and Physics*, *20*(13), 7753–7781. https://doi.org/10.5194/acp-20-7753-2020

Travis, K. R., Nault, B. A., Crawford, J. H., Bates, K. H., Blake, D. R., Cohen, R. C., et al. (2024). Impact of improved representation of volatile organic compound emissions and production of NO_x reservoirs on modeled urban ozone production. *Atmospheric Chemistry and Physics*, *24*(16), 9555–9572. https://doi.org/10.5194/acp-24-9555-2024

Watanabe, K., Yachi, C., Song, X. J., Kakuyama, S., Nishibe, M., & Michigami, S. (2017). Measurements of atmospheric hydroperoxides at a rural site in central Japan. *Journal of Atmospheric Chemistry*, *75*(1), 71–84. https://doi.org/10.1007/s10874-017-9362-z

Weinstein-Lloyd, J. B., Lee, J. H., Daum, P. H., Kleinman, L. I., Nunnermacker, L. J., Springston, S. R., & Newman, L. (1998). Measurements of peroxides and related species during the 1995 summer intensive of the southern oxidants study in Nashville, Tennessee. *Journal of Geophysical Research*, *103*(D17), 22361–22373. https://doi.org/10.1029/98JD01636

Wofsy, S. C., Afshar, S., Allen, H. M., Apel, E. C., Asher, E. C., Barletta, B., et al. (2018). ATom: Merged atmospheric chemistry, trace gases, and aerosols (version 1.5) [Dataset]. *ORNL Distributed Active Archive Center*. https://doi.org/10.3334/ORNLDAAC/1581

Woo, J.-H., Kim, Y., Kim, H.-K., Choi, K.-C., Eum, J.-H., Lee, J.-B., et al. (2020). Development of the CREATE inventory in support of integrated climate and air quality modeling for Asia. *Sustainability*, *12*(19), 7930. https://doi.org/10.3390/su12197930

Yang, L. H., Jacob, D. J., Colombi, N. K., Zhai, S., Bates, K. H., Shah, V., et al. (2023). Tropospheric NO_2 vertical profiles over South Korea and their relation to oxidant chemistry: Implications for geostationary satellite retrievals and the observation of NO_2 diurnal variation from space. *Atmospheric Chemistry and Physics*, *23*(4), 2465–2481. https://doi.org/10.5194/acp-23-2465-2023

Zhai, S., Jacob, D. J., Pendergrass, D. C., Colombi, N. K., Shah, V., Yang, L. H., et al. (2023). Coarse particulate matter air quality in East Asia: Implications for fine particulate nitrate. *Atmospheric Chemistry and Physics*, *23*(7), 4271–4281. https://doi.org/10.5194/acp-23-4271-2023

Zhang, Q., Liu, J., He, Y., Yang, J., Gao, J., Liu, H., et al. (2018). Measurement of hydrogen peroxide and organic hydroperoxide concentrations during autumn in Beijing, China. *Journal of Environmental Sciences*, *64*, 72–81. https://doi.org/10.1016/j.jes.2016.12.015

Zhang, X., He, S. Z., Chen, Z. M., Zhao, Y., & Hua, W. (2012). Methyl hydroperoxide (CH_3OOH) in urban, suburban and rural atmosphere: Ambient concentration, budget, and contribution to the atmospheric oxidizing capacity. *Atmospheric Chemistry and Physics*, *12*(19), 8951–8962. https://doi.org/10.5194/acp-12-8951-2012

Zheng, B., Tong, D., Li, M., Liu, F., Hong, C., Geng, G., et al. (2018). Trends in China's anthropogenic emissions since 2010 as the consequence of clean air actions. *Atmospheric Chemistry and Physics*, *18*(19), 14095–14111. https://doi.org/10.5194/acp-18-14095-2018

Zheng, J., Alaouie, A., Weinstein-Lloyd, J. B., Springston, S. R., & Nunnermacker, L. J. (2002). Measurement of hydroperoxides during the Texas 2000 air quality study. In *Fourth conference on atmospheric chemistry: Urban, regional and global scale impacts of air pollutants* (pp. 218–223). American Meteorological Society.